Role of the wetting layer for the SiGe Stranski–Krastanow island growth on planar and pit-patterned substrates

2011 Semicond. Sci. Technol. 26 014028

(http://iopscience.iop.org/0268-1242/26/1/014028)

Semicond. Sci. Technol. **26** (2011) 014028 (5pp) doi:10.1088/0268-1242/26/1/014028

Role of the wetting layer for the SiGe Stranski–Krastanow island growth on planar and pit-patterned substrates

J J Zhang[1,3], A Rastelli[2], O G Schmidt[2] and G Bauer[1]

[1] Institute of Semiconductor and Solid State Physics, University Linz, A-4040 Linz, Austria
[2] Institute for Integrative Nanosciences, IFW Dresden, Helmholtzstr. 20, D-01069 Dresden, Germany

E-mail: j.zhang@ifw-dresden.de

Received 14 June 2010, in final form 5 August 2010
Published 9 December 2010
Online at stacks.iop.org/SST/26/014028

Abstract
We investigate the homogeneity and thickness of a Ge wetting layer (WL) both on planar and pit-patterned Si(0 0 1) substrates by utilizing a combination of atomic force microscopy and selective chemical etching. On planar substrates, the WL is thinner or Si richer around the islands, while on the patterned ones it is thinner on the pit sidewall regions. On planar substrates, a substantial amount of Ge is transferred from the WL to the islands at the initial stage of island formation, while on patterned substrates this scenario is not observed due to the fact that islands form within the pits before the WL reaches the critical thickness on the planar surface in the regions between the pits. The WL thickness increases with increasing Ge deposition after island formation both on planar and patterned substrates, caused by Si–Ge intermixing in the WL at a relatively high growth temperature. By using the WL as etch-stop, we use the same etching solution to investigate the shape of buried SiGe islands.

(Some figures in this article are in colour only in the electronic version)

According to the Stranski–Krastanow growth model, in strained layer heteroepitaxy, island formation may occur on top of a wetting layer (WL), whereby elastic energy is released [1, 2]. The Si/SiGe system with a lattice mismatch of about 4% is considered a typical one for this kind of growth instability, and numerous investigations have been devoted to the studies of its morphological evolution. For the growth of Ge on flat Si substrates, Tersoff [3] has shown that the layer-by-layer growth is stabilized up to about $n = 3$ Ge monolayers because of the reduction of the strain energy associated with surface dimerization. Later on, detailed first principles calculations were performed [4–6] which demonstrated that the surface energy decreases with the number n for typical low energy $(N \times M)$ reconstructions and reaches a limiting value for n at about 5. Also, Si–Ge intermixing during WL formation and evolution has been widely investigated [7–11].

For the Ge growth on pit-patterned Si substrates atomic force microscopy (AFM) experiments have shown, that no homogeneous Ge WL is formed within the pits [12]. After the deposition of a Si buffer layer, the pits typically have the shape of inverted, truncated or multifaceted pyramids [12, 13]. The Ge wetting layer exhibits a more complex kind of ripple morphology which consists of {1 0 5} and {0 0 1} facets before the onset of Ge island formation in the center of the pits [12]. Prism-shaped ripples are bounded by {1 0 5} facet, and at the intersections at the pit corners a kind of staircase consisting of {0 0 1} and {1 0 5} facets appears. The formation of this morphology is driven by surface energy minimization and elastic strain relaxation.

While the average properties of the WL (its thickness and composition) have been investigated by different experimental techniques, such as photoluminescence and x-ray scattering methods [6, 14–16] possible lateral variations of these properties are generally difficult to access.

Selective wet chemical etching combined with scanning probe microscopy has recently emerged as a simple and powerful tool to study the properties of SiGe nanostructures with high spatial resolution [17–23]. Among different etching solutions, Wang *et al* found that the NH_4OH solution (10%

[3] Presently at Institute for Integrative Nanosciences, IFW Dresden, Helmholtzstr. 20, D-01069 Dresden, Germany.

NH_4OH at 75 °C) selectively etches Si over $Si_{1-x}Ge_x$ [24] and later Rosenblad *et al* showed that the potassium hydroxide solution is a proper etchant for etching Si over $Si_{1-x}Ge_x$ [25]. Schmidt *et al* found that a diluted H_2O_2 solution (31% H_2O_2) etches $Si_{1-x}Ge_x$ with $x > 65\%$ over Si [17], and Stoffel *et al* [26] and Katsaros *et al* [18] further demonstrated that NHH solution (1:1 vol. (28% NH_4OH):(31% H_2O_2)) selectively etches $Si_{1-x}Ge_x$ over pure Si with $x > 10\%$ and shows an exponentially increasing etching rate with increasing Ge fraction x [18], no preferential etching direction and a negligible dependence on strain [26].

In this paper, the NH_4OH solution has been used for qualitatively determining the homogeneity and thickness of the Ge WL on planar and pit-patterned Si(0 0 1) substrates. Our etching results show that the WL is actually inhomogeneous after island formation. On planar substrates the WL is preferentially etched in regions around SiGe islands, while on pit-patterned substrates it is preferentially etched in the pit sidewalls, indicating a thinner WL in these preferentially etched regions. Moreover, on patterned substrates, the etching results clearly show that pits are preferential positions for deposited Ge. On planar substrates, a substantial amount of Ge is transferred from the WL to islands during the initial stages of island formation. However, this phenomenon is not observed on patterned substrates. Furthermore, by using the WL as an effective etch-stop for the NH_4OH solution, we investigate the shape of embedded islands capped with Si at different temperatures.

The samples were grown by solid-source molecular beam epitaxy (MBE), and two-dimensional pit arrays with a period of 800 nm were patterned by electron beam lithography and reactive ion etching. After *ex situ* chemical cleaning, the samples were dipped in a diluted HF solution to create a hydrogen-terminated surface before loading into the MBE chamber. After *in situ* outgassing and Si buffer growth, different Ge amounts (from 2 to 15 monolayers (ML)) were deposited both on planar and pit-patterned Si(0 0 1) substrates at a substrate temperature of 720 °C and at a rate of 0.03 Å s^{-1}. After growth, the samples were cooled to room temperature, extracted from the MBE chamber and immediately etched in 10% NH_4OH solution at 75 °C. This solution selectively etches Si over $Si_{1-x}Ge_x$. Its selectivity increases with the Ge fraction x and is more than 80:1 even for $Si_{0.9}Ge_{0.1}$ while the etching rate decreases with increasing x [24]. The reason why we are using the NH_4OH solution instead of the potassium hydroxide solution is that the former shows a better selectivity in comparison to the latter [24, 27]. The surface morphology was investigated using AFM in the tapping mode.

Figures 1(*a*) and (*b*) show the AFM images of a sample obtained by depositing 8 ML Ge at 720 °C on a planar substrate and etched in the NH_4OH solution for 33 s and 36 s, respectively. After etching for 33 s, the Si substrate under the trenches surrounding the SiGe islands [28, 29] is slightly etched, while in the planar regions between islands it is not etched. This result indicates that the Ge WL is not able to protect the underlying Si substrate in the regions under the trenches. Our results also show that in regions around pyramid-shaped islands, where no trenches are observed [28],

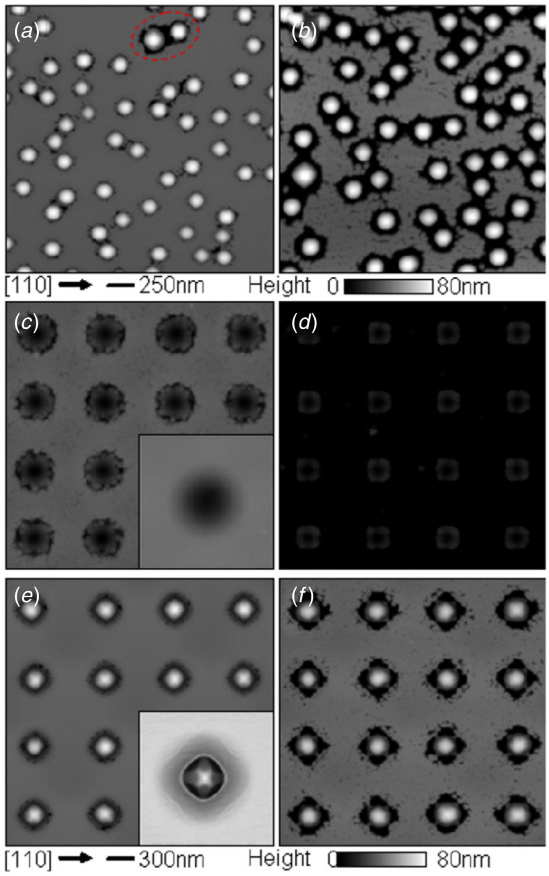

Figure 1. AFM images of: a sample obtained by depositing 8 ML Ge on a planar Si(0 0 1) substrate and etched for 33 s (*a*) and 36 s (*b*); a sample with 2 ML Ge on a patterned Si(0 0 1) substrate etched for 5 s (*c*) and 10 s (*d*); a sample with 6 ML Ge on a patterned substrate etched for 26 s (*e*) and 29 s (*f*) in the NH_4OH solution at 75 °C. The insets in (*c*) and (*e*) show as-grown unit cells after 2 ML Ge and after 6 ML Ge, respectively. The Ge was deposited at 720 °C, and the patterned substrates have a pit period of 800 nm.

the substrate is also preferentially etched (not shown here). After additional etching for 3 s, the substrate under the WL in the planar regions is also etched and deep trenches are observed around SiGe islands, as shown in figure 1(*b*). Since the etching rate of $Si_{1-x}Ge_x$ decreases with increasing x, the preferentially etched regions indicate a thinner or Si richer WL. In principle, the local compressive strain present at the island perimeters could also locally enhance the etching rate. We will however provide additional evidence below that the preferential etching mainly reflects local inhomogeneities of the WL thickness or Si content. The appearance of deep trenches in figures 1(*a*) and (*b*) is thus ascribed to a local depletion of Ge, since the compressive stress produced by the islands at their base perimeters makes these regions unfavorable for the incorporation of Ge [30, 31]. Furthermore, strain induces enhanced Si–Ge intermixing [32, 33]. This explanation is further supported by the results shown in figure 1(*a*) (see islands marked by the dashed ellipse): Si is preferentially removed in regions between closely spaced islands, due to a larger compressive strain [34, 35]. However, the difference in the 'critical time' for the etching solution to reach the Si substrate in regions around islands and in between islands is

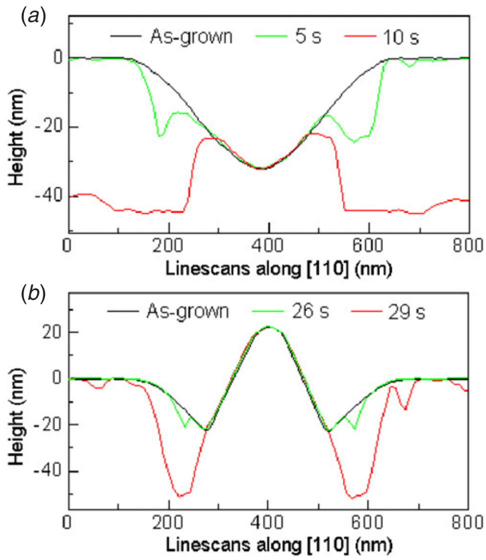

Figure 2. AFM linescans along the [1 1 0] direction passing through: (*a*) pit centers for representative SiGe-filled pits shown in the inset of figure 1(*c*) (as-grown), in figure 1(*c*) (5 s) and in figure 1(*d*) (10 s); (*b*) island centers for representative SiGe islands shown in the inset of figure 1(*e*) (as-grown), in figure 1(*e*) (26 s) and in figure 1(*f*) (29 s).

only about 3 s, indicating that the WL inhomogeneity on the surface is rather small. This finding is in qualitative agreement with the results of continuum simulations performed by Tu and Tersoff [36]: a SiGe WL is present all over the Si surface but shows a local thinning around islands.

Figures 1(*c*) and (*d*) show AFM images of a sample obtained by growing 2 ML Ge at 720 °C on a patterned Si substrate with a period of 800 nm and etched for 5 and 10 s, respectively. The inset in figure 1(*c*) shows an AFM image of the pit morphology (one unit cell) prior to etching. The shape changes occurring during etching are illustrated by AFM linescans passing through the pit centers along the [1 1 0] direction in figure 2(*a*). After 5 s etching, the regions of the pit close to the surrounding planar surface (pit sidewalls) are preferentially etched, while the planar surface between pits begins to be attacked by the etching (note the roughness in figure 1(*c*), which is not present prior to etching). After 10 s etching, the Si substrate has been deeply etched (by a few tens of nanometers) except under the bottom of the SiGe-filled pits, where the WL is still able to protect the underlying Si. These results clearly indicate that the WL is strongly inhomogeneous. Specifically, the pit centers are covered by a larger Ge amount than other regions, since they represent minima of the chemical potential for Ge incorporation.

Further, we investigate the WL homogeneity after island formation on patterned substrates. Figures 1(*e*) and (*f*) show AFM images of a sample with 6 ML Ge etched for 26 and 29 s, respectively. The inset in figure 1(*e*) shows an AFM image of an island located at the center of a pit prior to etching. The shape changes are further illustrated by AFM linescans passing through the island centers along the [1 1 0] direction in figure 2(*b*). After 26 s etching, the Si under the pit sidewalls is preferentially etched, and after 29 s etching the Si under

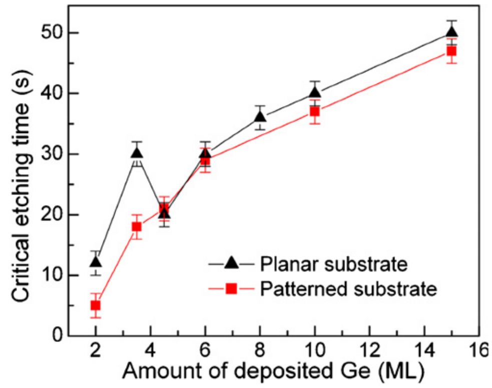

Figure 3. Critical etching time as a function of deposited Ge amount at 720 °C on planar and pit-patterned Si(0 0 1) substrates with a period of 800 nm. The etching was performed in the NH_4OH solution at 75 °C. The critical etching time is defined as the time needed for the solution to reach the Si below the WL.

the planar surface between pits also starts being removed. As seen from the AFM linescan after 26 s etching in figure 2(*b*), the preferentially etched regions on the pit sidewalls are more than 40 nm away from the island boundaries and the compressive strain induced by islands on these regions is negligible [37]. Therefore, we ascribe the preferential etching of the Si substrate under the pit sidewalls to a reduced WL thickness, which possibly originates from the terraced structures on the pit sidewalls [12] as seen in the inset of figure 1(*e*).

We now focus on the evolution of the WL during Ge deposition by measuring the critical etching time, which is defined as the time elapsed until the Si(0 0 1) substrate under the planar surfaces begins to be etched, as shown in figures 1(*b*), (*c*) and (*f*). Figure 3 displays the critical etching time for the WL both on planar and pit-patterned Si substrates as a function of deposited Ge amount from 2 to 15 ML. We see that, on planar substrates, the critical etching time, namely the WL thickness, first increases before island formation, then decreases when island growth sets in (from 3.5 to 4.5 ML) and then monotonically increases with further Ge deposition. In contrast, on pit-patterned substrates, the critical etching time increases monotonically with increasing Ge deposition.

On planar substrates, Ge is transferred from the WL into the islands at the initial stages of island formation (from 3.5 to 4.5 ML), similarly to previous measurements by photoluminescence [6, 14, 15] and x-ray scattering methods [16]. On pit-patterned substrates, as mentioned above, pits are preferential sites for the deposited Ge atoms. Therefore, for a given amount of deposited Ge, the thickness of the WL on the areas away from the pits is lower than that on planar substrates before island formation. This explains the difference in critical etching times for Ge amounts up to 3.5 ML (see figure 3). After the deposition of 3.5 ML Ge, an ordered array of pyramids forms in the patterned pits and, interestingly, no Ge transfer from the WL into islands is observed. We ascribe this observation to the reduced thickness of the WL on the planar surface in between the pits: the Ge in the rather thin WL well below the critical thickness for island formation stays in the WL instead of going to the islands. Therefore, at

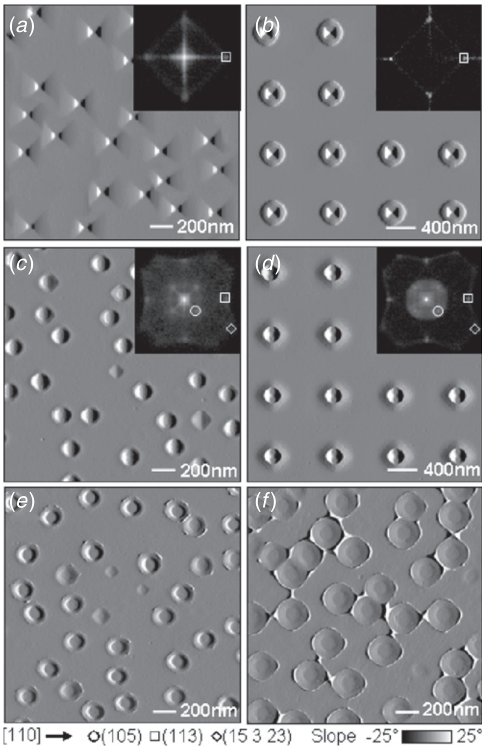

Figure 4. AFM images of samples obtained after deposition of 5 ML Ge at 720 °C capped with 30 nm Si at 500 °C prior to etching (*a*), (*b*) and after selective etching of the cap layer for 20 s in the NH_4OH solution (*c*), (*d*) for islands on planar (*a*), (*c*) and patterned (*b*), (*d*) substrates. (*e*) and (*f*) AFM images of samples obtained after selective etching of the cap layer for 20 s in the NH_4OH solution for islands grown on planar substrates (5 ML Ge at 720 °C) capped with 30 nm Si at 620 °C and 720 °C.

the initial stages of island formation on patterned substrates, no Ge material is transferred from the WL into the islands.

Before island formation, the critical etching time increases rapidly as a function of deposited Ge, while after the island formation it increases gradually, both on planar and patterned substrates. The former indicates that the WL growth is energetically favorable before reaching the critical value for island formation. The latter indicates that the WL thickness keeps increasing upon Ge deposition or that the WL becomes Ge-richer, which was also observed by the photoluminescence study at relative high growth temperatures [14]. In fact we expect significant Si–Ge intermixing between the deposited Ge and the Si in the substrate during the deposition process, because of the relative high growth temperature used here.

As far as the WL thicknesses and their local variation on patterned substrates are concerned, we note that these properties strongly depend on the pit sizes, shapes and periods. For instance, for patterned pits with a smaller period as used in [12, 22, 23], where no flat regions between islands are observed, the WL is thinner on the pit sidewalls (as seen here) and also on ridge positions between islands [23].

The fact that the NH_4OH solution etches the WL very slowly (see figure 3) allows us to use the WL as 'etch-stop' to investigate the shapes of embedded SiGe islands capped at different temperatures by selective removal of the Si cap. Figures 4(*a*) and (*b*) show the AFM images of samples obtained after 5 ML Ge at 720 °C capped with 30 nm at 500 °C on planar and patterned Si(0 0 1) substrates, and correspondingly (c) and (d) show the AFM images of the disclosed islands after 20 s etching in NH_4OH. After 30 nm Si cap at 500 °C, we clearly see pyramid-shaped islands with {1 1 3} facets as demonstrated by surface orientation maps [38] in the insets of figures 4(*a*) and (*b*), similarly to the previous reports for islands capped at low temperatures [39]. After 20 s in the NH_4OH solution, the 30 nm Si cap is completely etched away, while the WL acts as an etch stop, and the underlying Si is not attacked. We see that on the planar substrate, there is a bimodal island shape distribution with pyramids and domes, while on the patterned substrate islands are uniformly dome-shaped [13]. The direct comparison between figures 4(*a*) and (*c*) and between figures 4(*b*) and (*d*) shows that the surface morphology of pyramid-shaped structures is not related to the shape of buried islands and that the pits are partially filled during the Si capping. Moreover, the {1 0 5} facets are still clearly seen on the disclosed islands and no changes are observed between them (figures 4(*c*) and (*d*)) and the as-grown islands without Si cap (not shown here), indicating negligible shape changes and intermixing during the Si capping at such a low temperature.

Figures 4(*e*) and (*f*) show the AFM images of disclosed islands obtained after 20 s etching in NH_4OH for islands grown on planar substrates (5 ML Ge at 720 °C) capped with 30 nm Si at 620 °C and 720 °C. The comparison between figures 4(*c*), (*e*) and (*f*) shows that the height of the disclosed islands decreases whereas their width increases with capping temperature. At higher capping temperatures (620 °C and 720 °C) they display a clear top (0 0 1) surface. These changes are further demonstrated by AFM linescans along [1 1 0] direction, passing through the centers of the disclosed islands capped at the three different temperatures, as shown in figure 5. Moreover, we see that after the 20 s etching in the NH_4OH solution the underlying Si around the islands is not attacked if the islands are capped with Si at 500 °C, while it is etched a few nanometers if capped at 620 °C and 720 °C. We attribute this finding to significant Si–Ge intermixing occurring during Si capping at high temperatures [9]. For such conditions, both the WL and the islands get intermixed with the deposited Si atoms. As a result, the high aspect ratio islands are destabilized and the Ge WL gets more diluted with Si, resulting in the system evolving toward an energetically preferred alloyed SiGe quantum well [36].

In summary, we have reported on the observation of inhomogeneities of the SiGe WL both on planar and patterned Si(0 0 1) substrates by using selective etching with a NH_4OH solution. On planar substrates the WL is thinner or Si richer around the islands, while on the patterned ones it is thinner on the pit sidewall regions. On planar substrates, a substantial amount of Ge is transferred from the WL to the islands at the initial stage of island formation, while on patterned substrates this scenario is not observed since islands form in the pits before the WL reaches the critical thickness on the planar parts in between the pits. After island formation, the WL thickness increases with increasing Ge deposition both on

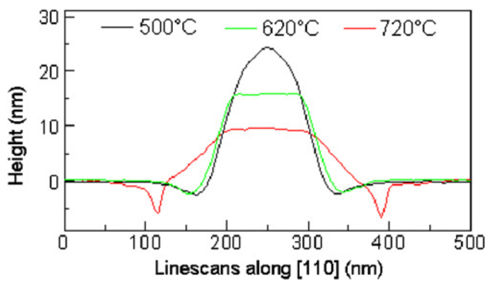

Figure 5. AFM linescans passing through island centers along the [1 1 0] direction for typical islands shown in figures 4(*c*), (*e*) and (*f*).

planar and patterned substrates. The detailed investigation of shape changes of embedded islands capped at different temperatures demonstrates that both the WL and the islands get intermixed with the deposited Si atoms at relatively high capping temperatures.

Acknowledgments

This work was supported by the FWF (SFB025, IRON) Vienna and by the EC project d-DOTFET. The authors acknowledge M Brehm and F Schäffler for helpful discussions.

References

[1] Shchukin V A, Ledentsov N N and Bimberg D 2003 *Epitaxy of Nanostructures* (Berlin: Springer)
[2] For a review see e.g. Stangl J, Holý V and Bauer G 2004 *Rev. Mod. Phys.* **76** 725
[3] Tersoff J 1991 *Phys. Rev.* B **43** 9377
[4] Beck M J, Van de Walle C and Asta M 2004 *Phys. Rev.* B **70** 205337
[5] Lu G H, Cuma M and Liu F 2005 *Phys. Rev.* B **72** 125415
[6] Brehm M *et al* 2009 *Phys. Rev.* B **80** 205321
[7] Tu Y H and Tersoff J 2004 *Phys. Rev. Lett.* **93** 216101
[8] Qin X R, Swartzentruber B S and Lagally M G 2000 *Phys. Rev. Lett.* **84** 4645
[9] Rastelli A, von Känel H, Albini G, Raiteri P, Migas D B and Miglio L 2003 *Phys. Rev. Lett.* **90** 216104
[10] Malachias A, Metzger T H, Stoffel M, Schmidt O G and Holy V 2007 *Thin Solid Films* **515** 5587
[11] De Seta M, Capellini G and Evangelisti F 2008 *Phys. Rev.* B **77** 045431
[12] Chen G, Lichtenberger H, Bauer G, Jantsch W and Schäffler F 2006 *Phys. Rev.* B **74** 035302
[13] Zhang J J, Stoffel M, Rastelli A, Schmidt O G, Jovanović V, Nanver L K and Bauer G 2007 *Appl. Phys. Lett.* **91** 173115
[14] Schmidt O G, Lange C and Eberl K 1999 *Appl. Phys. Lett.* **75** 1905
[15] Brehm M, Grydlik M, Lichtenberger H, Fromherz T, Hrauda N, Jantsch W, Schäffler F and Bauer G 2008 *Appl. Phys. Lett.* **93** 121901
[16] Schülli T U, Richard M I, Renaud G, Favre-Nicolin V, Wintersberger E and Bauer G 2006 *Appl. Phys. Lett.* **89** 143114
[17] Schmidt O G, Denker U, Christiansen S and Ernst F 2002 *Appl. Phys. Lett.* **81** 2614
[18] Katsaros G *et al* 2006 *Surf. Sci.* **600** 2608
[19] Rastelli A, Stoffel M, Malachias A, Merdzhanova T, Katsaros G, Kern K, Metzger T H and Schmidt O G 2008 *Nano Lett.* **8** 1404
[20] Wu C C and Hull R 2006 *J. Appl. Phys.* **100** 083510
[21] Katsaros G, Stoffel M, Rastelli A, Schmidt O G, Kern K and Tersoff J 2007 *Appl. Phys. Lett.* **91** 013112
[22] Zhang J J, Rastelli A, Groiss H, Tersoff J, Schäffler F, Schmidt O G and Bauer G 2009 *Appl. Phys. Lett.* **95** 183102
[23] Zhang J J, Hrauda N, Groiss H, Rastelli A, Stangl J, Schäffler F, Schmidt O G and Bauer G 2010 *Appl. Phys. Lett.* **96** 193101
[24] Wang F, Shi Y, Liu J L, Lu Y, Gu S L and Zheng Y D 1997 *J. Electrochem. Soc.* **144** L37
[25] Rosenblad C, Deller H R, Dommann A, Schroeter T and von Känel H 1998 *J. Vac. Sci. Technol.* A **16** 2785
[26] Stoffel M, Malachias A, Merdzhanova T, Cavallo F, Isella G, Chrastina D, von Känel H, Rastelli A and Schmidt O G 2008 *Semicond. Sci. Technol.* **23** 085021
[27] Katsaros G 2006 *PhD Thesis* Universität Konstanz
[28] Denker U, Schmidt O G, Jin-Philipp N Y and Eberl K 2001 *Appl. Phys. Lett.* **78** 3723
[29] Kamins T I, Carr E C, Williams R S and Rosner S J 1997 *J. Appl. Phys.* **81** 211
[30] Tersoff J, Teichert C and Lagally M G 1996 *Phys. Rev. Lett.* **76** 1675
[31] Zhang J J, Zhang K W and Zhong J X 2004 *Surf. Sci.* **551** L40
[32] Schmidt O G, Denker U, Christiansen S and Ernst F 2002 *Appl. Phys. Lett.* **81** 2614
[33] Schmidt O G and Eberl K 2000 *Phys. Rev.* B **61** 13721
[34] Stoffel M, Rastelli A, Kiravittaya S and Schmidt O G 2005 *Phys. Rev.* B **72** 205411
[35] Vastola G, Gatti R, Marzegalli A, Montalenti F and Miglio L 2008 *Self-Assembled Quantum Dots* ed Zhiming M Wang (Berlin: Springer) p 421
[36] Tu Y and Tersoff J 2007 *Phys. Rev. Lett.* **98** 096103
[37] Vastola G, Montalenti F and Miglio L 2008 *J. Phys.: Condens. Matter.* **20** 454217
[38] Lutz M A, Feenstra R M, Mooney P M, Tersoff J and Chu J O 1994 *Surf. Sci.* **316** L1075
[39] Stoffel M, Rastelli A and Schmidt O G 2007 *Surf. Sci.* **601** 3052